Integrated modeling activities for the James Webb Space Telescope: optical jitter analysis

T. Tupper Hyde[a], Kong Q. Ha[b], John D. Johnston[a], Joseph M. Howard[a], Gary E. Mosier[a]
[a]NASA Goddard Space Flight Center, 8800 Greenbelt Road, Greenbelt, MD 20771
[b]Jackson and Tull, Chartered Engineering, 7375 Executive Place, Seabrook MD 20706

ABSTRACT

This is a continuation of a series of papers on the integrated modeling activities for the James Webb Space Telescope (JWST). Starting with the linear optical model discussed in part one, and using the optical sensitivities developed in part two, we now assess the optical image motion and wavefront errors from the structural dynamics. This is often referred to as "jitter" analysis. The optical model is combined with the structural model and the control models to create a linear structural/optical/control model. The largest jitter is due to spacecraft reaction wheel assembly disturbances which are harmonic in nature and will excite spacecraft and telescope structural. The structural/optic response causes image quality degradation due to image motion (centroid error) as well as dynamic wavefront error. Jitter analysis results are used to predict imaging performance, improve the structural design, and evaluate the operational impact of the disturbance sources.

Keywords: Jitter, dynamics, optical, integrated modeling, LOS, WFE, image quality, telescope

1. INTRODUCTION

JWST is a large infrared observatory to be launched in 2011. It features a telescope with a 6.5 meter deployed primary mirror of 18 segments, a suite of four science instruments, a spacecraft bus, and a large flexible sunshield. Figure 1 shows artwork of the current JWST design.

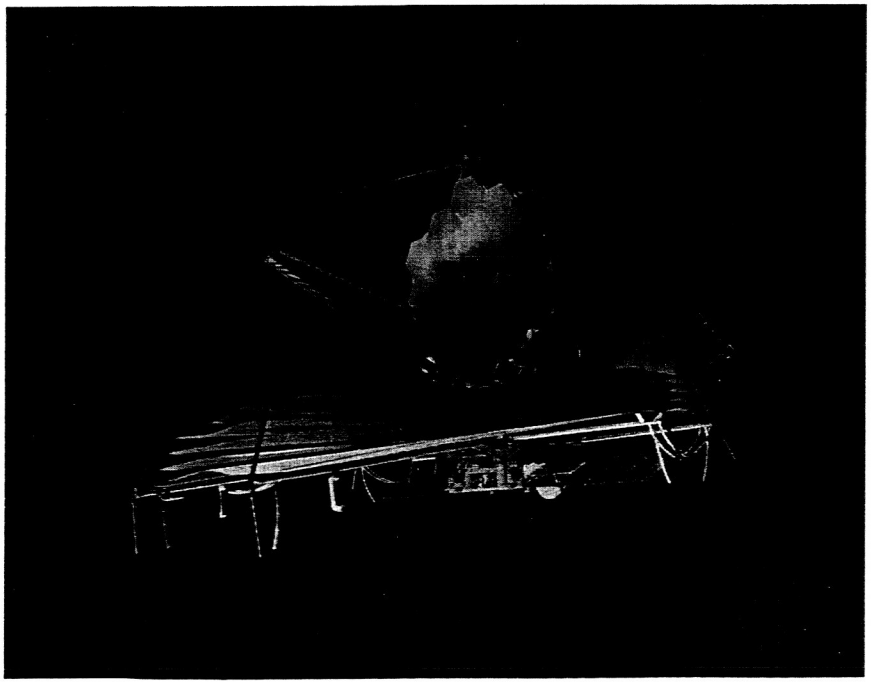

Figure 1: JWST (image courtesy NGST)

One of the unique challenges of JWST is the large, flexible nature of the deployed telescope. This brings with it the fact that the telescope cannot be fully tested on the ground. Much of the JWST performance, therefore, will be verified by modeling that is, in turn, validated by tests that can be performed on the ground. One of the key performance metrics is the image quality that is driven by wavefront error (WFE) and image motion. On the JWST project, the term jitter is used for both image motion and the dynamic WFE present during an exposure. Currently, the allocation for line of sight (LOS) motion and WFE from structural dynamics is 4 mas and 14 nm, respectively. The primary source for these errors is the motion of the structure supporting the optics being driven by dynamic disturbances on-board the observatory. The largest contributor to jitter is the vibration induced by the reaction wheel assemblies (RWAs). The RWAs on JWST reside in the spacecraft bus and produce unwanted forces and torques in the form of a set of sinusoids at frequencies related to the wheel spin speed. The unique structural dynamics design of JWST addresses the RWA-induced vibration transmission to the telescope through two stages of passive isolation: the RWAs rest on isolated mounts, and the entire telescope is structurally decoupled from the spacecraft bus and sunshield through the OTE tower isolator. This paper will trace the analysis of the RWA-induced jitter through disturbance, structure, control, and optics modeling.

The disturbance model of the RWA consists of a set of force and torque harmonics extracted from wheel test data. Each harmonic in the set has a frequency (a sub- or super- ratio of the wheel speed) and amplitude. The structural model is a traditional finite element model (FEM) that will grow in fidelity as the project gains design detail. The control model includes linear, continuous time, feedback compensators derived from the full non-linear, discrete time controller designs. The optics are modeled with a linear optic model (LOM) extracted from the full prescription of the telescope. The optics model includes design residual WFE and fully includes the effect of the segmented primary mirror. Finally, model uncertainty factors (MUFs) are applied multiplicatively to the transfer functions created by the combined disturbance, structural, and optical model. The MUFs represent the 1 sigma uncertainty in the predicted jitter; they are, effectively, error bars on the analysis. The MUF ratios are set by a schedule that starts with relatively high uncertainties for analysis only and lowers them as model fidelity is improved through component, subsystem, and system testing.

2. INTEGRATED MODELING ON JWST

Multi-disciplinary engineering analysis, or integrated modeling, is a critical element of the JWST mission. Primarily, integrated modeling supports engineering design and verification of high level optical requirements for image quality and sensitivity, or signal-to-noise ratio for faint objects. The image quality requirements are specified by Strehl ratio and encircled energy. Current plans for end-to-end optical performance verification rely on modeling to a degree surpassing previous programs. The final verification process requires modeling and analysis to correct for the effects of the optical test procedure, metrology, gravity, and thermal/seismic effects on opto-mechanical stability before extrapolation to behavior in the on-orbit environment. Figure 2 shows the coupled nature of the integrated modeling elements used on the JWST project.

The optical systems engineer maintains performance (error) budgets to control allocations to the various subsystems that comprise the JWST observatory. These budgets are traceable to the high level optical requirements. The image quality requirements are re-cast as requirements on wavefront error. These allocations may be roughly classified as belonging either to calibration – alignment and figuring – of the optics, or to opto-mechanical stability between periodic recalibrations. The sensitivity requirement is the basis for allocations to radiometric performance, stray light suppression, and detector performance.

One could view the primary integrated modeling activities as consisting of four distinct multi-disciplinary analysis efforts, three supporting verification of image quality requirements, and the fourth supporting verification of the sensitivity requirement. The analyses supporting verification of the image quality requirements are (1) wavefront sensing and control, to estimate the post-calibration alignment and figure errors, (2) thermal distortion, or STOP (Structural-Thermal-Optical), to estimate alignment figure drift due to observatory re-pointing and other transient factors, and (3) jitter, to estimate the blurring and distortion due to uncompensated pointing and vibration.

The applications of integrated modeling will change over the program life cycle. In the formulation and requirements definition phase, a strawman design was developed to address the high level mission requirements, goals, and constraints. The role of integrated modeling was to validate this design concept by showing that the conceptual design

met the requirements with margin, subject to reasonable assumptions, and that initial sub-allocations to observatory elements and sub-systems were also reasonable.

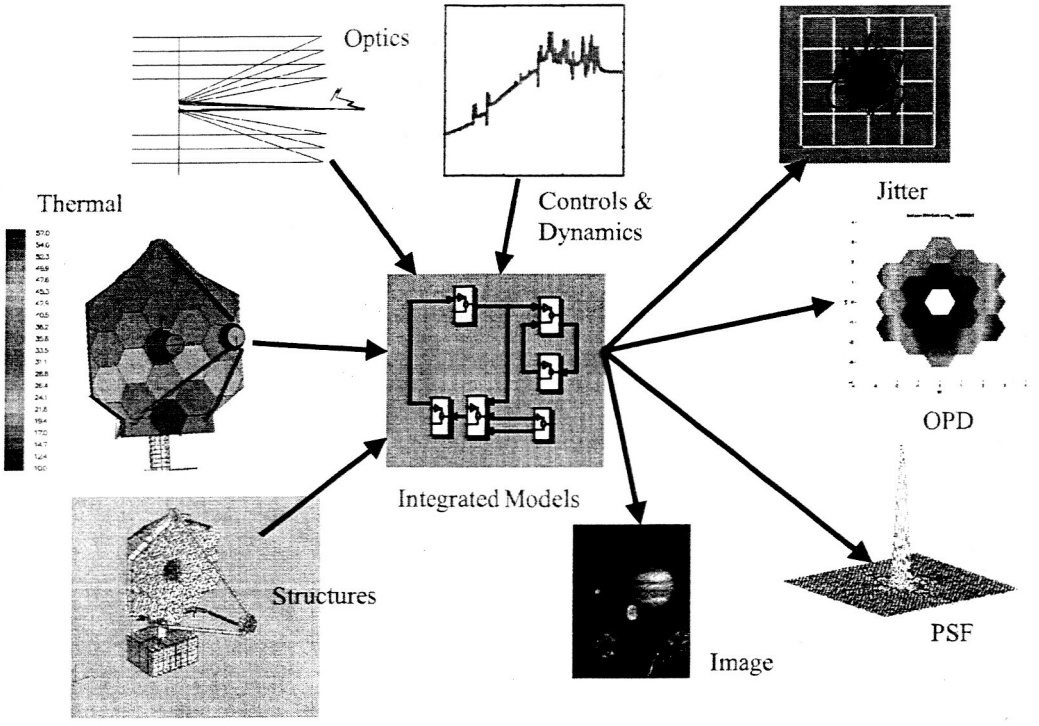

Figure 2: Integrated Modeling for JWST

Following a series of requirements reviews at the various program levels (mission, observatory, telescope, instruments), the modeling activity has aligned with the architecture/design activity in a series of cycles, of 6-9 month duration. There will be multiple design cycles between major program review milestones. At the beginning of each cycle, a baseline design (or several as long as significant design trades are active) will be "frozen", and the set of multi-disciplinary analyses will be executed to verify that the baseline design(s) for that cycle meet the optical system requirements, with margin. The analysis will not only produce predictions of nominal design performance, but will also address uncertainties in performance due to variability in design parameters, material properties, and the environment. In particular, for the jitter analysis, modeling uncertainties are addressed via Model Uncertainty Factors, or MUFs.

Model validation is critical, and will take different forms throughout the program life cycle. Initially, with the exception of heritage components (e.g. ACS sensors and actuators) and technology already developed for JWST (e.g. the passive vibration isolation system), models can only be validated by an independent analysis effort. Over time, as additional components are built or procured, and structure is built up, models will be anchored with testing. In this way, the MUFs will be reduced along with uncertainty in the ultimate performance of the observatory.

The results presented here are based on models representing the design at the time of the System Requirements Review.

3. JITTER ANALYSIS

3.1. Jitter analysis process map

The jitter analysis process begins with definitions of disturbance sources and performance metrics. For JWST, the jitter performance metrics are both image motion (centroid in two axes) RMS and dynamic WFE RMS over an exposure. An exposure can be anywhere between 12 and 10,000 seconds. The primary disturbance source of concern is the RWA-induced vibration, characterized by the wheel speed. The process creates an integrated control, structural, optical model

that provides a linear transfer function matrix between RWA-induced forces and torques to image motion and WFE. Frequency domain techniques are then used to assess the RMS image motion and WFE for a given wheel speed. The analysis results are plots of image motion and WFE as a function of wheel speed. MUFs are applied to account for the likely under prediction in the raw model. Peaks in the plot that are within the operating wheel speed range are then compared versus the allocated budgets. The process is summarized in the map of Figure 3.

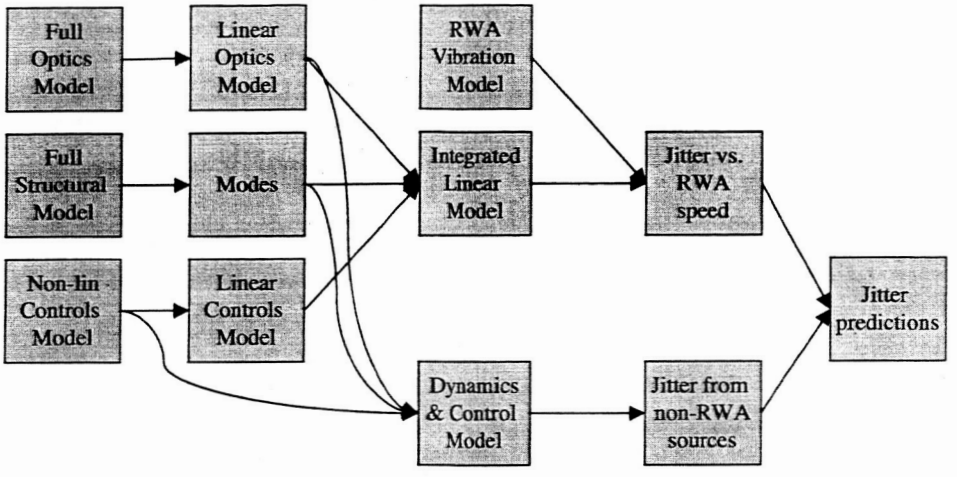

Figure 3: Jitter Analysis Process Map

The creation of the RWA vibration model from component test data is covered in section 3.2. Creation of reduced linear optical, structural, and control models from the more complete full, non-linear models is covered in sections 3.3-3.5. The integration of these models into a single linear model is followed by model reduction using a significant modes process and is described in section 3.6. Finally the jitter as a function of wheel speed is calculated and plotted in section 3.7. The separate analysis task of predicting image motion from non-RWA sources (sensor noises, actuator noises and resolutions, etc.) happens in parallel with the RWA vs. wheel speed analysis and the results are combined in the image motion budget. Finally the jitter predictions are compared to the budget and, if there is not significant margin, mitigaton techniques might be studied. These mitigations could include: reduced RWA operating speed range, damping augmentation, more isolation, or improved placement of critical modal frequencies. If it were just MUF gain that is causing the exceedance of the budget allocation, then additional or earlier testing to allow lower MUFs would be a reasonable mitigation.

3.2. Disturbance sources

Sources of jitter on JWST include mechanical vibrations, sensor and actuator noises and resolution, and slew residual. The focus of the current analysis is on the RWA-induced vibrations that are the dominant source of jitter. Other mechanism disturbances (antenna drive and science instrument filter wheels) are separately analyzed and can be mitigated by operational limits on their use during observations. Sensor and actuator noises and resolutions are also separately analyzed in time domain (non-linear simulation) or frequency domain (linear transfer function) to get their contributions. Slew residuals are analyzed in time domain and the time to settle to an acceptable jitter is included in the slew time budget.

The RWA disturbance consists of a set of sinusoidal forces and torques based on harmonics of wheel speed. Physically, these disturbances are due to slight imperfections in the bearing system of the RWA. The harmonic ratios are a define set based on bearing geometry and number of balls. For each harmonic, axial force, radial force, and radial torque eac are sinusoidal with amplitude that is proportional to the square of the wheel speed. The radial force rotates in the plan of the rotor at the harmonic frequency. The static and dynamic unbalance of the RWA rotor drives the amplitude of th 'once per rev' harmonic. Amplitudes of the other harmonics are determined by bearing imperfections and are determined from test data. After several RWAs of a given design have been tested, mean and standard deviation harmonic amplitude can be determined from the test data set. The mean amplitude is used in the model and the standa deviation is used for the MUF on disturbance gain. The RWA disturbance model for JWST is based on test data for

eight RWAs from the Chandra program. The RWA disturbance forces and torques are applied to the RWA nodes of the structural model. For time domain simulations, random phases for the axial force, radial force, and radial torque must be selected for each harmonic.

3.3. Structural model

The deployed observatory NASTRAN structural finite element model, Figure 4, includes flexible representations of the optical telescope element, integrated science instrument module, spacecraft, and a simplified sunshield. There are approximately 40000 degrees of freedom (DOFs) in the model. The JWST prime contractor (NGST) developed the model under contract to NASA and delivered it to the government team at the time of the System Requirements Review in December 2003. NASA verified that the delivered model passes basic validity checks and has subsequently used the model for linear dynamic analysis. Approximately 400 system modes were recovered in the 0 – 100 Hz frequency range with the model in a free-free support condition. The first flexible mode has a frequency of 0.4 Hz. There are several modes in the 0.4 – 4.0 Hz frequency range involving participation from the simplified sunshield and the optical telescope element (OTE) tower isolator. The RWA isolators have flexible modes starting around 7 Hz. The low frequency modes of the telescope structure involve bending of the secondary mirror support structure in the 7-9 Hz frequency range (Figure 5), twisting of the primary mirror backplane at 12 Hz (Figure 5), and 'flapping' of the primary mirror wings at 20 Hz.

The structures discipline provides frequencies, mode shapes, and modal damping values for use in integrated modeling and attitude control system studies. Mass normalized mode shapes are partitioned based on degrees of freedom corresponding to predefined input/output reference points in the model. In the present studies, the input DOFs correspond to RWA nodes where disturbances and control forces are applied. The output nodes are at optical locations required for performance analysis. Modal damping values are either uniform or variable. Variable modal damping values are based on group participation determined using modal strain energy fractions. This approach is used primarily to account for increased damping in the isolators relative to the remainder of the observatory. Both the OTE tower and RWA isolators have test-derived damping values in the range of 5% of critical damping. The spacecraft/sunshield is expected to exhibit damping levels typical of room temperature structures, while the cryogenic telescope and integrated science instrument module may have damping values an order of magnitude lower.

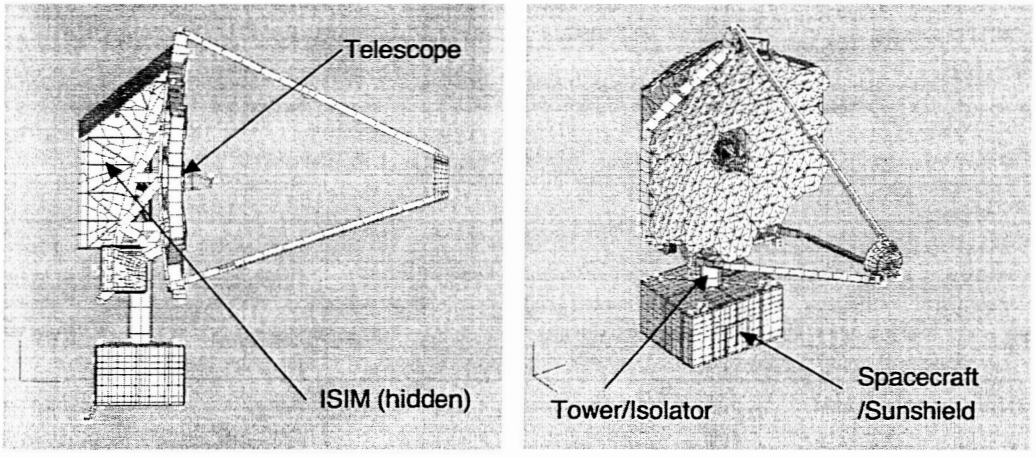

Figure 4: JWST Structural Model

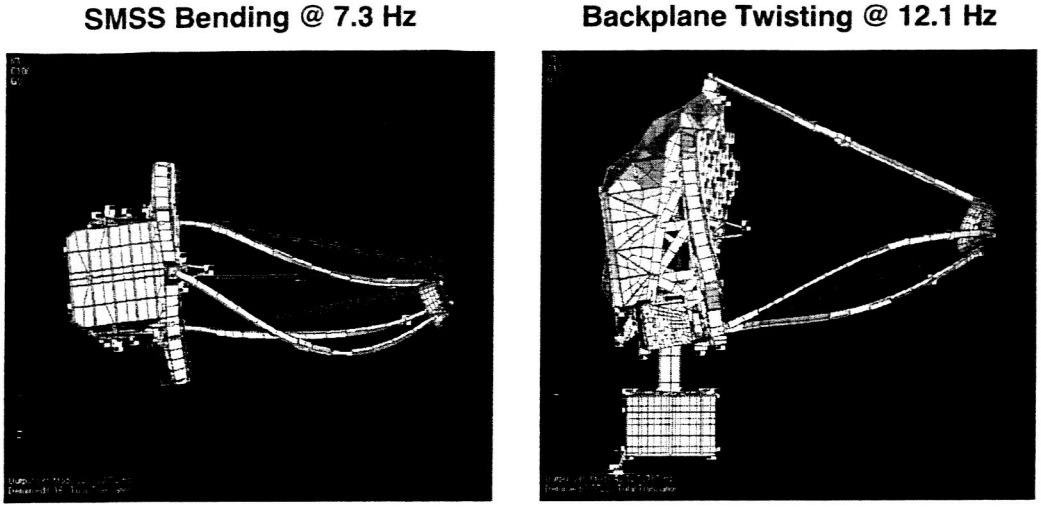

Figure 5: Two Representative Mode Shapes Critical to Jitter

Model uncertainty factors for the structural model are of two types: damping uncertainty and modal gain uncertainty. The damping uncertainty is a "knock-down" factor applied to the current best estimate (CBE) of the raw damping in each component of the structural model (RWA, RWA isolators, spacecraft/sunshield, tower isolator, telescope structure). The damping MUF is large for untested subsystems and improves as material, structural component, and subsystem damping tests are made in the program. The modal gain MUF is a multiplier to the modal response and, again, applied statistically to each subsystem so as to represent a +1 sigma "error bar" on the transfer function prediction. As with the damping MUF, the modal gain MUF starts large for untested subsystems and improves as component, subsystem, and system tests are conducted.

3.4. Optical model

The JWST optical model used for jitter analyses can be briefly described as a first-order Taylor expansion of the optical path lengths of a grid of rays traced through the system, uniformly spaced at the entrance pupil. The variables expanded upon are the rigid body degrees of freedom (DOF) for each optical component in the system. Naturally, this model is valid only when the perturbations are very small so that any higher order terms are negligible. This linear optical model be summarized in the following equation:

$$\mathbf{L} = \mathbf{L}_0 + \frac{\partial \mathbf{L}}{\partial \mathbf{U}} \Delta \mathbf{U} + O(2)$$

where $\mathbf{L}$ contains the optical path lengths of the grid of rays from the entrance pupil to the exit pupil, $\mathbf{L}_0$ contains the nominal (unperturbed) path lengths for the system, $\Delta \mathbf{U}$ represents the perturbation of the rigid body degrees of freedom, and $O(2)$ represents the second and higher order terms of the expansion which are disregarded for this linear analysis. The first-order derivative term, $\frac{\partial \mathbf{L}}{\partial \mathbf{U}}$, is constructed by perturbing each DOF, one at a time, and evaluating the change in pathlengths from the nominal for each case. This process is described in detail in Ref. 1. Note that this first-order derivative term contains all wavefront data including absolute piston, tip/tilt, and all higher-order terms, since it is evaluated with respect to the nominal reference sphere at the exit pupil without regard to chief ray motion. Wavefront error is defined here as the optical path length difference, or OPD, between the perturbed system and the nominal system where all pathlengths are equal to that of the chief ray. As such, the image motion of the system due to perturbations is captured since global tip/tilt has not been removed from the optical path. Since the error budget for JWST is divided into image motion (i.e. the tip/tilt term of wavefront), and wavefront error due to image motion (i.e. wavefront with tip/tilt removed), we separate the $\frac{\partial \mathbf{L}}{\partial \mathbf{U}}$ data into two matrices: $\frac{\partial \mathbf{C}}{\partial \mathbf{U}}$ and $\frac{\partial \mathbf{W}}{\partial \mathbf{U}}$, representing centroid motion sensitivities and wavefront error sensitivities, respectfully. The process used for this is described in an accompanying paper.

In summary, all ray tracing for the linear optical model is performed ahead of time to generate linear sensitivities which act as transfer functions converting rigid body motions of optical components to absolute image motion at the detector

and wavefront error induced due to the misaligned components. Comparing wavefront maps generated from the sensitivities to those generated by ray tracing show less than 1% difference for random realizations of perturbations of all components up to 1 micron or micro-radian motions or tilts, respectively.

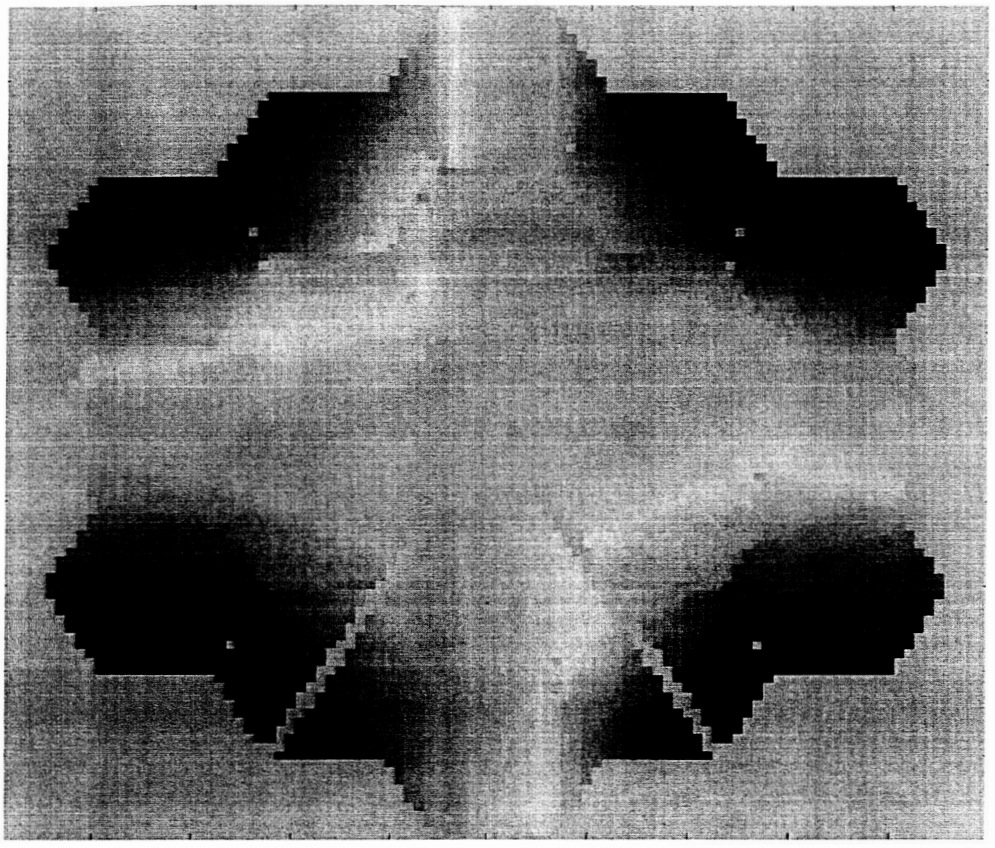

Figure 6: OPD map plot

The linear sensitivities are formatted in a matrix for ease of use and plotting. Figure 6 shows the WFE OPD map corresponding to the significant backplane twisting mode in the structural model at 12.1 Hz (Figure 5).

3.5. Control model

The pointing control system of JWST consists of a traditional attitude control system (ACS) and a focal plane based fine guidance loop. The ACS has a 0.02 Hz bandwidth and uses star trackers and gyros to control the spacecraft bus with RWA torques. The fine guidance loop uses a fine guidance sensor (FGS) based on a focal plane array near the main science instruments to provide centroid data on guide stars at 16 Hz. The fine guidance loop commands a fine steering mirror (FSM) in the optical train and is closed at about 1 Hz. Finally, a separate off-loading loop is used to add a slight command offset to the ACS loop to continuously bring the FSM back to the center of its range. Figure 7 shows the architecture of the JWST pointing control loops. The coarse-fine pointing control design for JWST has been largely unchanged from the early concept studies in 1996. For jitter analysis, the non-linear, time domain (Simulink) model of the three controllers (ACS, fine guiding, and offload) is converted to a linear, state-space description suitable for inclusion in the larger integrated jitter model. The jitter analysis task breaks neatly into two regimes. The RWA disturbance almost entirely excites structural modes above the bandwidth of any controller and could be done on the open loop model. The sensor and actuator noise contributions to jitter, correspondingly, are below the controller bandwidth and affect mostly the rigid body response.

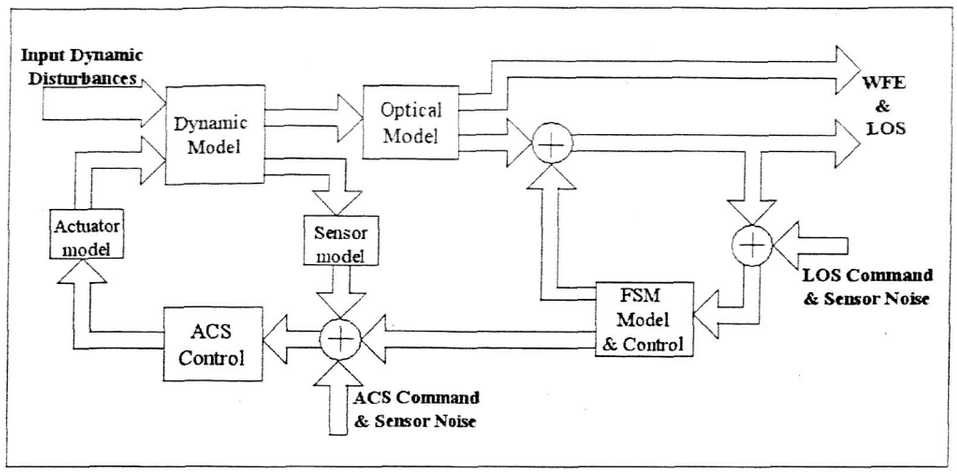

Figure 7: JWST Pointing Control Loops

3.6. Integrated structural/control/optics model

One of the major on-going activities in the integrated modeling effort has been the development of model-building tools. These tools are written in Matlab to implement algorithms and techniques to perform a variety of model-building functions. These functions include forming a dynamic model from finite element mode shape data, deriving linear optical model and sensitivity maps from ray-trace OPD data, and building system integrated models from the subsystem models. The modular coding of these tools provides the flexibility of producing integrated models with varying degrees of fidelity and complexity to efficiently support studies of different aspects of system performance. The range of models created go from relatively simple integrated models with an open-loop structure to evaluate jitter effects of high frequency disturbances to a more fully integrated model used to examine detailed aspects of system performance such as coupling between low-frequency disturbances and sensor noise. In the current JWST jitter analysis effort, integrated models generated are based on the general system configuration illustrated in Figure 7.

For most jitter analyses, continuous s-domain closed-form transfer functions are generated and used in representing the system. All the subsystems are modeled using the state space representation approach, and connected together according to design configuration, e.g. Figure 7. Time simulation can then be performed directly with the state space model to obtain time responses for specific input disturbance and/or sensor noise realizations. To derive frequency transfer functions for performance bound analysis, the state space model is numerically evaluated at a selected set of frequency points. For large order systems, this numerical approach avoids instabilities and round-off error induced in the root calculation that is required in the conversion between state space and closed form frequency transfer functions.

The selection of frequency points is based on specific integrated model and disturbance characteristics. It first considers the structural modes in the system, determines from the disturbance profile all possible resonant frequencies that can occur in the system response, and builds up the frequency set containing points that are sampled on and near the resonant frequencies based on second order response with given system damping factors.

For JWST, the structure of the state space representation of the integrated model can be shown to essentially compose as the following closed-loop form:

$$\begin{pmatrix} \dot{x}_1 \\ \dot{x}_2 \end{pmatrix} = \begin{pmatrix} A_1 + B_1 D_2 C_1 & B_1 C_2 \\ BC & A_2 + B_2 D_1 C_2 \end{pmatrix} \begin{pmatrix} x_1 \\ x_2 \end{pmatrix} + \begin{pmatrix} B_1 & 0 \\ 0 & B_2 \end{pmatrix} \begin{pmatrix} u_1 \\ u_2 \end{pmatrix}$$

$$\begin{pmatrix} y_1 \\ y_2 \end{pmatrix} = \begin{pmatrix} C_1 & 0 \\ 0 & C_2 \end{pmatrix} \begin{pmatrix} x_1 \\ x_2 \end{pmatrix} + \begin{pmatrix} D_1 & 0 \\ 0 & D_2 \end{pmatrix} \begin{pmatrix} u_1 \\ u_2 \end{pmatrix}$$

Where *[A1,B1,C1,D1]* and *[A2,B2,C2,D2]* are two models given in state space representation, connected in a closed-loop system. This form applies directly to the ACS block and the body dynamic block that are in series with sensor and actuator models, respectively. Output of this closed-loop portion is fed into the optical model block. For jitter analysis, the optical model contains linear sensitivity mappings that convert small motions at the optical nodes to perturbations in the LOS and WFE. The above closed-loop form also applies to a unity feedback that is formed with the FSM block, which contains the FSM dynamic and controller, and has LOS command and uncompensated LOS with perturbation as input. The same closed-loop form is used to connect these two portions of the configuration together to complete the integrated model. This implementation of the integrated model makes all the input and output from all the blocks in the system available to allow for computation of response of any input/output pair in the system, for input arbitrary control command, to inject noise and disturbance, and to observe system intermediate states. Figure 8 shows Bode plots for the transfer functions from the ACS sensor noise and reaction wheel disturbance to the uncompensated and compensated LOS. With the ACS bandwidth of 0.02Hz, sensor noise below this bandwidth is passed through the system with unity gain, and with a PID controller, the low-frequency component of the disturbance can be seen to roll off as frequency approaches zero. Improvement shown in these plots of the compensated LOS over the uncompensated LOS is due to the FSM controller.

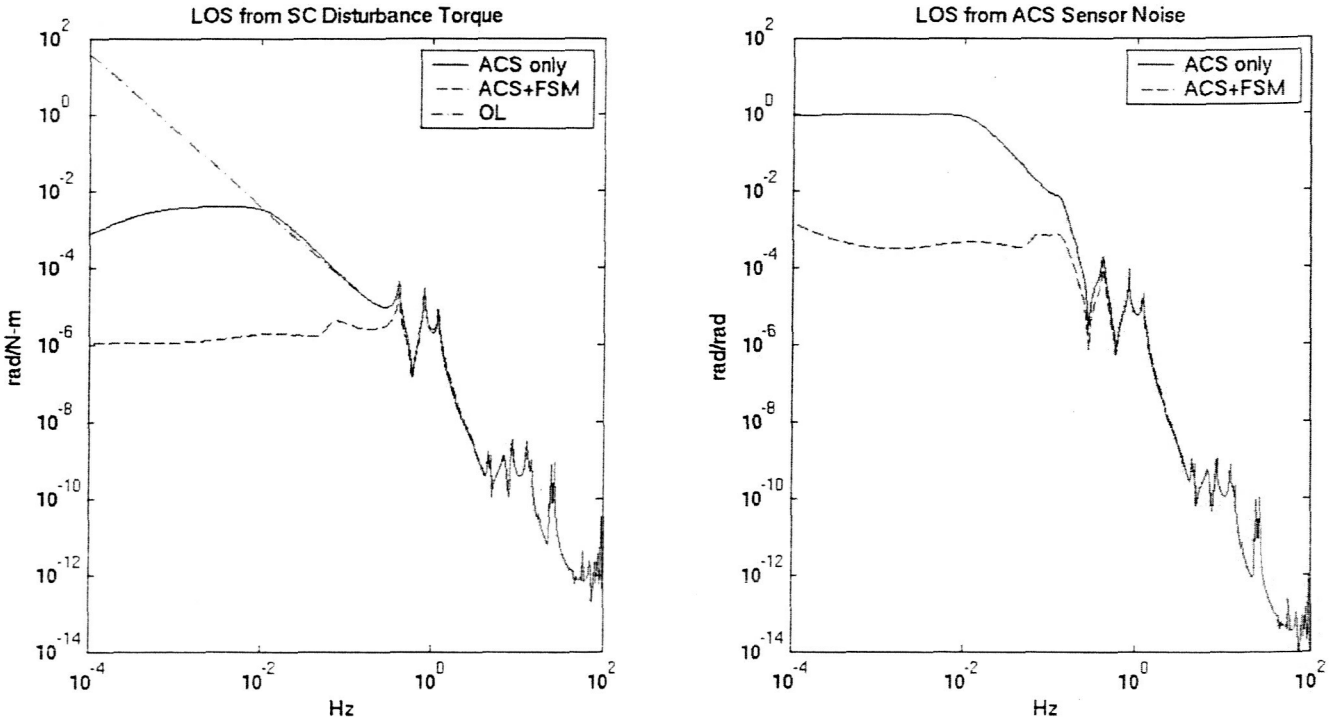

Figure 8: Bode Plots

In addition to deriving performance metrics such as LOS error, Strehl Ratio, and encircled energy from compensated LOS and WFE derived from the integrated model, various linear sensitivity analyses can also be performed to verify control design performance and stability requirements. By using the alternative closed-loop form that has the system matrix in the form *(A+BKC)* for some *[A,B,C]* and constant gain *K* that brings out the linear structure in different parts of the system (e.g. controller, optical sensitivity, dynamic parameters), the developed integrated model can support various sensitivity studies.

For JWST, a fully integrated model has more than 30 possible input signals ranging from spacecraft attitude and rate commands, to sensor noise, to various input disturbances, and it also has over 150 output signals including motions at all optical nodes, and intermediate signals from controllers and subsystem models. For a moderate level of fidelity, the model can contain over 400 states. With this size of model, jitter analyses to determine system performance in terms of LOS and WFE can be very intensive. To reduce the system order and ease computational burden, significant mode

selection of the structural dynamics must be performed. Structural modes that have negligible contribution to the jitter performance are identified and truncated.

For the reaction wheel static and dynamic imbalance disturbance, whose spectral content consists of harmonics that change with wheel speed, structural mode reduction is strongly recommended for the jitter analysis since the computation of performance metrics is somewhat more complex with reaction wheel speeds as an additional parameter. As wheel speed varies, typically 0-6000 RPM, the harmonic frequencies vary linearly, and their amplitudes vary with the square of the wheel speed. In normal operation, reaction wheel disturbance harmonics will sweep over all structural modes of frequency up to 100 Hz. This means high frequency modes cannot be ignored as is typically done due to the rigid body roll-off attenuation effect.

In order to minimize the computation time, the analysis process performs two steps to achieve the objective. It first selects significant structural modes based on the magnitude of only the flexible effective mass contributions over all input/output node pairs considered in the analysis. It then identifies and removes wheel speeds that do not have harmonics with frequencies coincide with significant modes. Figure 9 describes the jitter analysis process for the reaction wheel disturbance.

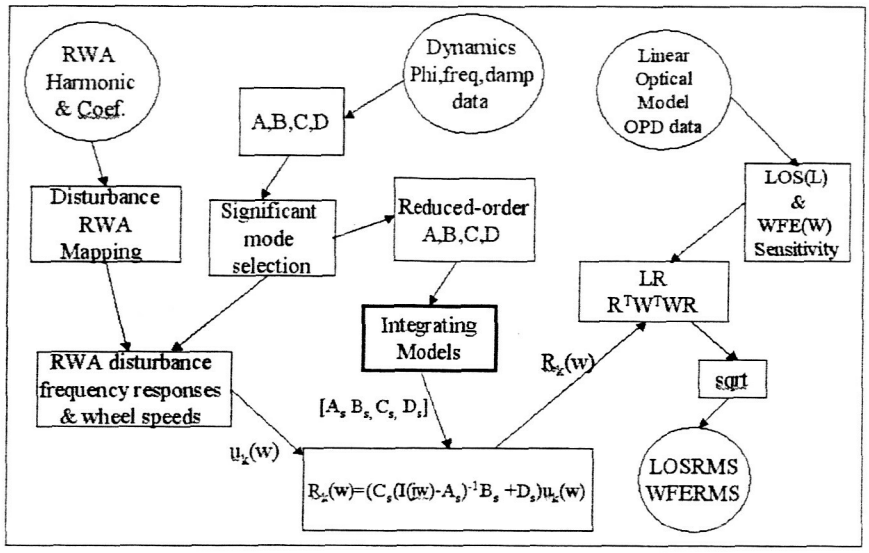

Figure 9: RWA disturbance jitter analysis calculations

The selection of significant modes is performed with modal eigenvectors. Typically, the selection is based on both the rigid and flexible effective mass contributions, however, since the rigid portion varies purely as the rigid roll-off effect, hence, as mentioned above, its contribution should not be taken into account in selecting significant modes. The flexible effective mass contribution of a given mode k is simply given by:

$$\frac{\tilde{\Phi}_{kO}\tilde{\Phi}_{kI}^{T}}{2\xi_k}$$

Where:

$\tilde{\Phi}_{kO}$ = Eigenvector associated with structural mode k, and all the output nodes

$\tilde{\Phi}_{kI}^{T}$ = Eigenvector associated with structural mode k, and all the input nodes

ξ_k = Damping factor associated with structural mode k.

For the reaction wheel disturbance, with the roll-off effect removed, there are more modes being retained in the set of significant modes as shown in Figure 10 (a-b).

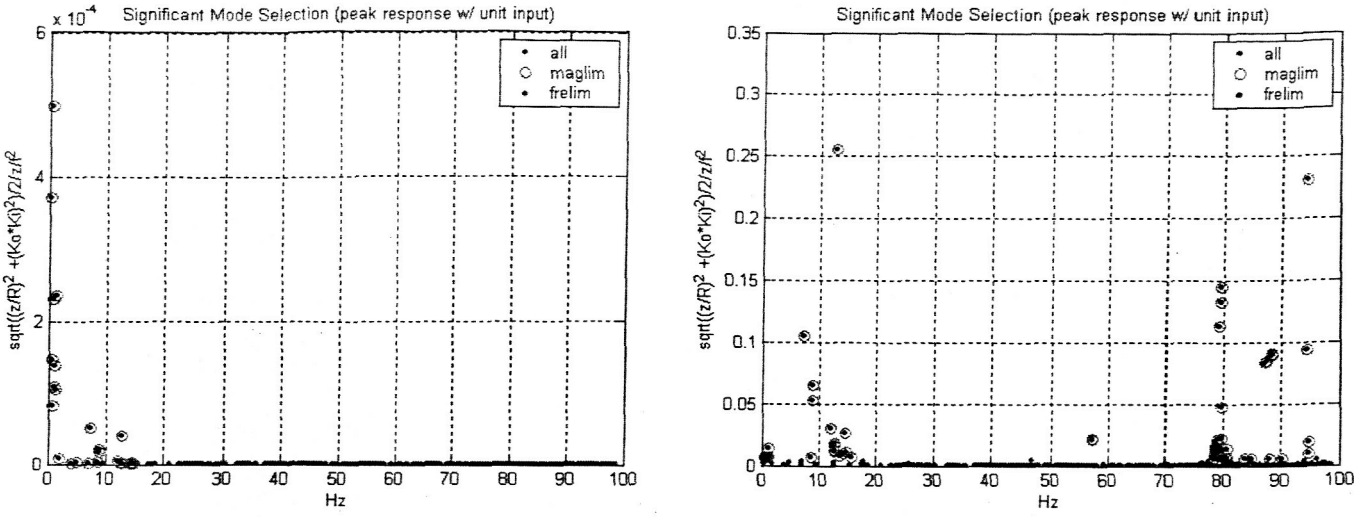

Figure 10: Mode selection with (a) and without (b) rigid mass contribution

3.7. Jitter versus RWA speed plots

The plots of LOS RMS and WFE RMS versus wheel speed (in revolutions per second (RPS)) are generated based on the RWA harmonic disturbances and the transfer function from RWA disturbance to optical response to include the MUFs. The net MUFs (including RWA disturbance, RWA isolator, SC structure, tower isolator, OTE structure, and optics) are 1.9 below 20 Hz ramping up to 3.9 at 40 Hz and above at this point in the program. The MUFs will be reduced as additional testing and model validation occurs over the coming years. Since some testing of subsystems has already occurred, the MUFs are already lower than they would be for a "pure analysis" case. Figures 11 and 12 show the results.

These plots were created by taking an evenly spaced sweep of wheel speeds and augmenting that wheel speed vector with a set of additional speeds that were calculated so that every harmonic "hits" every significant mode. This ensures that the maximum "peaks" in the resulting plot accurately pick out the wheel harmonic on structural response points. The analysis proceeds by looping over wheel speeds and calculating the LOS and WFE response from each harmonic. The result is multiplied by the square root of two to allow for the case where two (of the six) RWAs should happen to both reside simultaneously on the same structural mode (but in quadrature phasing with each other). The RSS of the response of the harmonics is then taken and plotted for that wheel speed point.

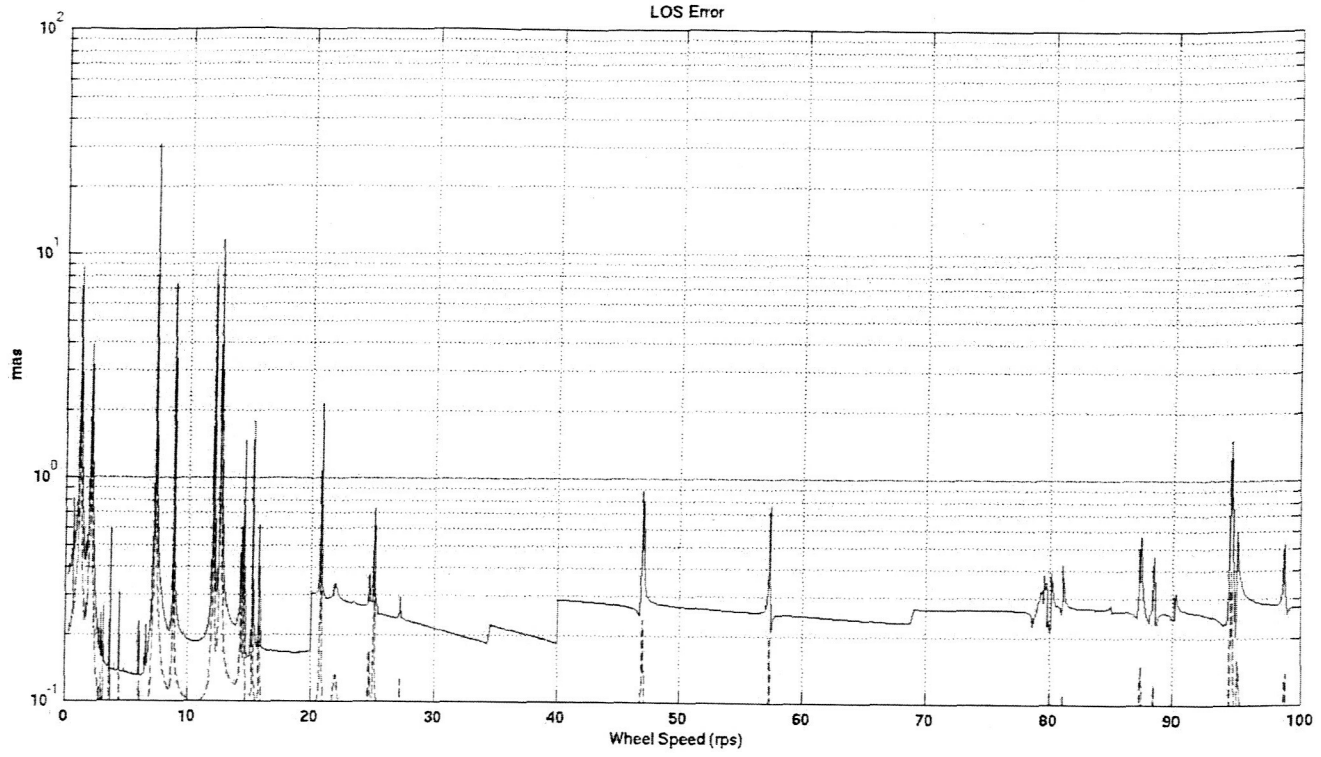

Figure 11: Image motion RMS versus wheel speed plot

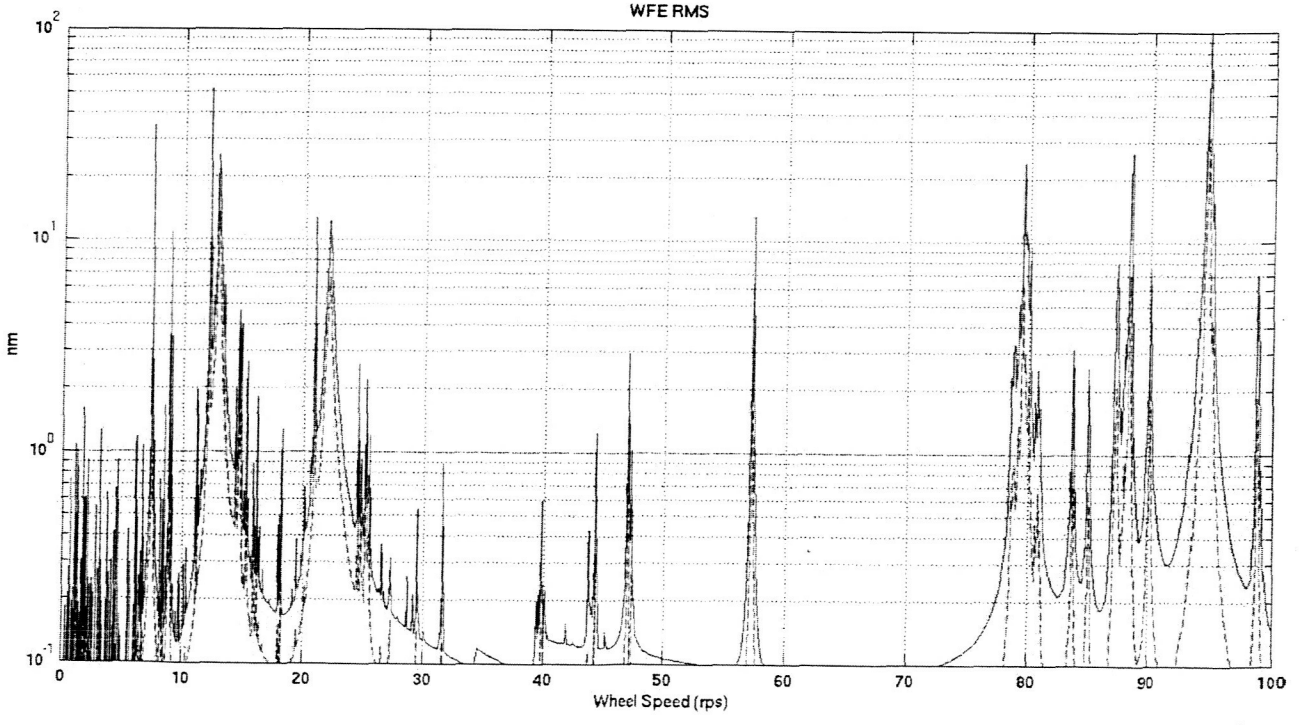

Figure 12: WFE RMS versus wheel speed plot

4. IMPLICATIONS FOR DESIGN AND OPERATION OF JWST

As RWA-induced jitter is an important element in the performance of JWST, the analysis predictions are used to drive options for design and operation of the observatory. Comparing Figures 11 and 12, one sees that the image motion performance, although exceeding the allocated 4 mas at several places below 13 Hz, is not as much of a problem as the WFE contribution to image degradation. The WFE RMS is predicted to exceed the allocated budget of 14 nm at several wheel speed ranges. The area at 12 RPS is mainly from the 'once per rev' imbalance of the wheels exciting lightly damped telescope modes at 12 (see Figure 5). The peak near 22 RPS is from a wheel subharmonic exciting the 12 Hz modes. Near 79 and 88 RPS, the wheels are exciting the modes of the individual segments moving against the backplane structure. Then, also from Figure 11, one can see that there is a large range of wheel speeds for which jitter does not exceed the allocation. The obvious mitigation for the RWA-induced jitter for JWST is to require the RWAs only to be operated between 15 and 75 RPS. Other possible mitigations include damping augmentation to the telescope, more aggressive isolation, better RWA balance, or modal tuning. It is also very important to remember that these predictions include net MUFs of up to 3.9. An attractive alternative to possibly lower the jitter predictions is to add or accelerate testing. This will have the effect of more accurately "grounding" the model and lowering the MUFs that are applied. Certainly for tests of damping in telescope materials and structural components, the cost versus risk decision is favorable toward conducting the tests. Good (and reasonably conservative) damping assumptions are very important as the very lightly damped telescope structure is driving the results; being off by a factor of two in damping assumption directly equates to a factor of two in predicted jitter.

In summary, the optical jitter for the JWST program is predicted with an integrated modeling process that combines disturbance, structural, optical, and control models. Model uncertainties are addressed through the use of MUFs to bound the one sigma predictions. Image motion and WFE prediction as a function of wheel speed are used to assess the benefits of structural design, damping, disturbance mitigation, and RWA operating speed limits.

REFERENCES

1. Joseph M. Howard, "Optical modeling activities for the James Webb Space Telescope (JWST) project: I. The linear optical model," Proc. SPIE Int. Soc. Opt. Eng. 5178, 82 (2004).
2. Johnston, J., et al, "Integrated modeling activities for the James Webb Space Telescope: Structural-Thermal-Optical Analysis," SPIE-5487-123.
3. Mosier, G., Parrish, K., Femiano, M., Redding, D., Kissil, A., Papalexandris, M., Craig, L., Page, T., and Shunk, R., "Performance Analysis Using Integrated Modeling", NGST Monograph No. 6, August 2000
4. Mosier, G., Femiano, M., Ha, K., Bely, P., Burg, R., Redding, D., Kissil, A., Rakoczy, J. and Craig, L., „An Integrated Modeling Environment for Systems-level Performance Analysis of the Next Generation Space Telescope,‰ SPIE Vol. 3356, Space Telescopes and Instruments V, 1998
5. Mosier, G., Femiano, M., Ha, K., Bely, P., Burg, R., Redding, D., Kissil, A., Rakoczy, J. and Craig, L., „Fine Pointing Control for a Next Generation Space Telescope,‰ SPIE Vol. 3356, Space Telescopes and Instruments V, 1998